# Wafer-level near zero field spin dependent charge pumping: effects of nitrogen on 4H-SiC MOSFETs

Mark A. Anders[1, a *], Patrick M. Lenahan[2, b] and J. T. Ryan[1, c]

[1]National Institute of Standards and Technology, 100 Bureau Drive, Gaithersburg, MD 20878, USA

[2]Penn State University, 101 EES Building, University Park, PA 16802, USA

[a]mark.anders@nist.gov, [b]pmlesm@engr.psu.edu, [c]jason.ryan@nist.gov

**Keywords:** NO anneal, near zero field spin dependent charge pumping, defects

**Abstract.** In this work, we describe a new way to measure spin dependent charge capture events at metal-oxide-semiconductor field-effect transistor interfaces (MOSFET) called near-zero-field spin dependent charge pumping (NZF SDCP) which yields similar information as conventional electron paramagnetic resonance. We find that nitric oxide post oxidation anneals have a significant effect on the spectra obtained from 4H-silicon carbide MOSFETs. We also likely resolve hyperfine interactions which are important for defect identification. Finally, we fully integrate a NZF SDCP measurement system into a wafer prober for high throughput applications.

## Introduction

Electron paramagnetic resonance (EPR) and electrically detected magnetic resonance (EDMR) have unrivaled ability to identify defects in silicon carbide (SiC) and SiC devices [1]–[6]. These techniques can directly identify the atomic scale defects connected to performance and reliability. However, these measurements typically require capital equipment such as a large electromagnet (around 350 mT), a cooling system, and a complicated microwave system. Off-the-shelf EPR/EDMR spectrometers can cost hundreds of thousands of dollars. EDMR also often requires sample dicing and wire bonding, which is not acceptable in a high-throughput environment. Consequently, we present a new technique called near zero field spin dependent charge pumping (NZF SDCP) which can extract similar information as EPR and EDMR without the need for a large electromagnet or complicated microwave system. As such, this technique is uniquely positioned for very simple integration within a wafer probe station, similar to the work of McCrory *et al.* who built and demonstrated a wafer-level EDMR spectrometer [7]. Their work paves the way for wafer-level EDMR measurements in high throughput environments. However, the EDMR technique, no matter the form factor, still requires an oscillating magnetic field. For the case of a traditional EDMR spectrometer, the oscillating magnetic field is introduced via microwaves in a resonance cavity or an RF coil. For the case of the wafer-level system, they are introduced via a small, fragile shorted coaxial probe (probe wire diameter 50 μm) [7]. The NZF measurement does not involve an oscillating magnetic field, thus does not require microwave or RF peripherals. The only requirement is a small (around 30 mT) linearly varying magnetic field.

In this work, we develop the basic NZF SDCP technique by comparing spectra of MOSFETs with and without post oxidation anneals (POA) in nitric oxide (NO). The atomic scale physics of NO POA at the MOSFET interface has previously been studied by EDMR [3], [8]–[10], thus a comparison can give insight into the physical mechanisms involved in the NZF SDCP response. For this case, we utilize ultra-low resonance frequency (ULRF) EDMR measurements which are made at 370 MHz resonance frequency in order to measure both the NZF and EDMR SDCP responses. We then build and demonstrate a wafer-level NZF spectrometer for high-throughput applications.

NZF SDCP detects spin dependent events such as charge capture in the current produced by the charge pumping (CP) measurement [11], [12]. CP is a powerful electrical measurement used to characterize channel/gate dielectric interface traps in MOSFETs, but does not yield information about

their chemical nature. The CP process, in the most straightforward approach, involves grounding the source and drain while applying a continuous trapezoidal waveform to the MOSFET gate in order to alternately invert and accumulate the interface, filling and emptying traps at the interface region. The waveform repeats at some frequency called the charge pumping frequency ($f_{CP}$). For an n-MOSFET, the low voltage level is chosen such that it accumulates the interface (less than flat band voltage) which fills interface traps with holes from the body. The high voltage level is chosen such that it inverts the interface (greater than threshold voltage) which fills the interface traps with electrons from the source and drain. The cycle repeats and the low pulse voltage again brings in holes from the body that recombine with the trapped electrons. The rise and fall times of the waveform are chosen to give adequate time for excess holes/electrons to diffuse back to their respective sources. The CP process results in a net change in recombination current measured at the body called the charge pumping current ($I_{CP}$) which is given by [11], [12]:

$$I_{CP} = q f_{CP} A_{eff} \overline{D_{it}} \Delta E_{CP}, \tag{1}$$

where $q$ is the electronic charge, $f_{CP}$ is the frequency of the trapezoidal gate pulse, $A_{eff}$ is the effective channel area (the area of the channel which is made to invert and accumulate), and $\overline{D_{it}}$ is the mean density of interface states within the measured band gap energy window ($\Delta E_{CP}$). $\Delta E_{CP}$ is nearly symmetric about mid gap and can be estimated by:

$$\Delta E_{CP} = 2k_B T \ln\left(\frac{\Delta V_G}{\overline{v_{th}}\, n_i \sqrt{\sigma_n \sigma_p}(V_{TH}^{CP} - V_{FB}^{CP}) \sqrt{t_r t_f}}\right), \tag{2}$$

where, $k_B$ is Boltzmann's constant, $T$ is temperature, $\Delta V_G$ is the gate waveform pulse amplitude, $\overline{v_{th}}$ is the geometric average of the electron and hole thermal velocity, $\sqrt{\sigma_n \sigma_p}$ is the geometric average of the electron and hole capture cross sections, $n_i$ is the intrinsic carrier concentration, $V_{TH}^{CP}$ and $V_{FB}^{CP}$ are the CP threshold and flatband voltages, respectively, and $t_r$ and $t_f$ are the rise and fall times of the gate waveform, respectively.

As previously mentioned, NZF SDCP is closely related to SDCP, the EDMR measurement [3], [13]. Since the physical mechanisms involved in EDMR are much better understood, we compare NZF and EDMR measurements in order to learn more about the NZF response. The underlying difference between the NZF SDCP and EDMR SDCP measurements is that EDMR utilizes an oscillating magnetic field to induce EPR transitions while the NZF measurement does not rely on resonance. For the simple case of EDMR of an electron in free space, resonance occurs when electromagnetic radiation with energy $E_{ph} = h\nu$ equals that of the electron Zeeman energy splitting $E = g_e \mu_B B$ (the photon is absorbed by the electron). Here, $h$ is Planck's constant, $\nu$ is the electromagnetic radiation frequency, $g_e$ is the free electron $g$ factor ($g_e$= 2.0023193…), $\mu_B$ is the Bohr magneton, and $B$ is the magnetic field. Simply, the electron spin state "flips" when absorbing the photon. For the case of an electron experiencing only spin-orbit coupling and electron-nuclear hyperfine interactions (a good approximation for the EDMR spectra involved in this work), the electron Hamiltonian is given by:

$$\mathcal{H} = \mu_B \boldsymbol{B} \bullet \boldsymbol{g} \bullet \mathbf{S} + \sum_i \mathbf{I}_i \bullet \boldsymbol{A_i} \bullet \mathbf{S}. \tag{3}$$

Here, $\mu_B$ is the Bohr magneton, $\boldsymbol{B}$ is the applied magnetic field vector, $\mathbf{S}$ is the electron spin operator, and $\mathbf{I}_i$ is the nuclear spin operator for the $i^{\text{th}}$ nucleus. $\boldsymbol{g}$ and $\boldsymbol{A_i}$ are essentially tensors which describe a defect's local environment and are usually referred to as the $g$ and $A$ tensors. Spin-orbit coupling causes the $g$ tensor components to deviate from the free electron $g_e$, and $A$ provides a

measure of electron-nuclear hyperfine interactions. The electron-nuclear hyperfine interaction spectra are very important for defect identification, often called the defect "fingerprint". Analysis of resonance spectra in terms of equations of this form allows definitive identification of the physical and chemical nature of defects.

EDMR exploits electron paramagnetic resonance and the spin dependence of charge capture. The seminal work of Kaplan-Solomon-Mott (KSM) explains this spin dependence [14]. The spin dependence of recombination comes from the formation of intermediate spin-pair states between a conduction band electron and a deep paramagnetic defect is spin dependent. For our case, the defects involved can be energetically located throughout the great majority of the band gap, as calculated by Eq. 2. Before recombination, the spin pair enters an intermediate state. If the pair is in a triplet configuration, they dissociate, and the intermediate pair is broken. If the pair is in a singlet configuration, they relax to the ground state; the electron becomes trapped. Recombination takes place when a hole is captured (typically fast). EPR increases the singlet-triplet ratio and thus enhances the recombination rate and recombination current. To measure SDCP via EDMR, a CP measurement is made on a MOSFET while simultaneously being exposed to RF radiation via a resonance coil while a small magnetic field that is slowly swept through resonance. The change in $I_{CP}$ is measured as a function of the magnetic field.

The NZF SDCP response is also due to charge capture events at the interface, but their recombination rate is altered by the mixing of singlet and triplet states, not EPR. At small magnetic fields, the singlet and triplet states can mix via hyperfine interactions. Because the singlet probability alters the capture cross section term in Eq. 2, we then modify $\sqrt{\sigma_n \sigma_p}$ to be $\sqrt{\sigma_n' \rho_S \sigma_p}$ where $\sigma_n'$ and $\sigma_p$ are the spin independent electron and hole capture cross sections, respectively. $\rho_S$ modifies the electron capture cross section while the hole capture cross section is assumed to always be spin independent. The mixing can change the singlet probability and change the recombination rate.. The spin Hamiltonian for a spin pair in a magnetic field can be written:

$$\mathcal{H} = \mathcal{H}_0 + \mathcal{H}_{S-T}, \tag{4}$$

where

$$\mathcal{H}_0 = \frac{1}{2}\mu_B(g_1 + g_2)(\boldsymbol{S}_1 + \boldsymbol{S}_2) \bullet \boldsymbol{B} - J(r)\left(\frac{1}{2} + 2\boldsymbol{S}_1 \bullet \boldsymbol{S}_2\right), \tag{4a}$$

$$\mathcal{H}_{S-T} = \frac{1}{2}\mu_B(g_1 - g_2)(\boldsymbol{S}_1 - \boldsymbol{S}_2) \bullet \boldsymbol{B} + \left(\sum_{j=0}^{m} a_{1,j}\boldsymbol{I}_j \bullet \boldsymbol{S}_1 + \sum_{k=0}^{n} a_{2,k}\boldsymbol{I}_k \bullet \boldsymbol{S}_2\right). \tag{4b}$$

Here, $\boldsymbol{S}_1$ and $\boldsymbol{S}_2$ are the spins of the free electron and paramagnetic defect, $g_1$ and $g_2$ are their $g$ values, $\boldsymbol{I}_1$ and $\boldsymbol{I}_2$ are the nuclear spins of their host atoms, $a_1$ and $a_2$ are their hyperfine parameters, and $\boldsymbol{B}$ is the magnetic field. The first term of $\mathcal{H}_0$ leads to the Zeeman splitting of the three triplet energy levels by $g\mu_B B$ and the second term separates the singlet and triplet states. $\mathcal{H}_{S-T}$ leads to the mixing of the singlet and triplet states via the hyperfine fields. At zero magnetic field, the singlet and three triplet states can mix. On increasing the magnetic field, the hyperfine field is suppressed, and less spin mixing between singlets and triplets occurs. This in turn reduces recombination events. This is not exactly the case for NZF SDCP, but this theory may still provide a basis for understanding our results. Because the response involves hyperfine interactions, we can learn about these important interactions with NZF SDCP. To measure the NZF SDCP effect, a CP measurement is made on a MOSFET placed in a small magnetic field which is slowly swept through zero Gauss. The change in $I_{CP}$ is measured as a function of the magnetic field. The NZF response may be affected by experimental parameters such as magnetic field sweep time and sweep direction, however we must form a better understanding of NZF SDCP in order to determine the effect, if any, of these parameters.

## Experimental

Our NZF and EDMR SDCP measurements were made on either a traditional custom-built NZF/EDMR spectrometer or a non-traditional wafer-level spectrometer. The traditional spectrometer consists of an electromagnet with 6 nested Helmholtz coils, a Kepco BOP 100-4M power supply, a Lake Shore Cryotronics 450 temperature-compensated Gaussmeter and Hall probe, and a computer which provides magnetic field control and data acquisition. The wafer-level system consists of a Signatone 1160 series manual wafer probe station, manipulators, DC probes made from semi-ridged coax cable (center conductors exposed), digital camera, a 75 mm diameter single-coil sweep electromagnet with a single 35 mm diameter nested modulation coil, a Kepco BOP 20-10D power supply, and a computer which provides magnetic field control and data acquisition. In both cases, we utilize lock-in detection by amplitude modulating the quasi-static magnetic field at audio frequency, thus we measure the approximate derivative of the NZF and EDMR response. Data shown as an "absorption" or integral was numerically integrated from the measured response. The gate waveform is applied with a Tabor Electronics WW2572A waveform generator. For all measurements, the trapezoidal gate waveform with a 50% duty cycle and a 100 ns rise and fall time was utilized. All measurements were made at room temperature. ULRF SDCP measurements were made on the traditional electromagnet, and resonance was induced via a Doty Scientific surface coil and resonance circuit (resonance frequency around 370 MHz). In all cases, current was measured on a Stanford Research Systems SR750 current preamplifier.

Two types of planar n-channel 4H-SiC MOSFETs were mainly studied. One had a 50 nm as-grown oxide with area (L x W) 1 x 424 $um^2$ with an effective channel mobility of about 1 $cm^2/Vs$, and the other had a 50 nm oxide which received a post oxidation anneal in NO at 1175 $^oC$ for 2 hours and had a gate area of (L x W) 1 x 1000 $um^2$ with an effective channel mobility of 31 $cm^2/Vs$. Both were grown on p-type epilayers. A third n-channel 4H-SiC MOSFET was used for demonstration of the wafer-level NZF SDCP set-up. It had a 10 nm $SiO_2$/ 30 nm $Si_3N_4$/ 10 nm $SiO_2$ gate stack and had a gate area of (L x W) 4 x 250 $um^2$ with an effective channel mobility of about 2 $cm^2/Vs$

Taking into account the accuracy of the Gaussmeter (0.002 mT), the accuracy of the current preamplifier used to measure the EDMR current, the accuracy of DAQ used to meassure the output voltage, and the signal-to-noise ratio (>100), our measurements of the relative magnetic field have an uncertainty no more than 0.03%, and our current measurements have an uncertainty no more than 0.01%.

## Results and Discussion

Fig. 1 is NZF and EDMR SDCP measurements from both samples. The responses around 13.7 mT and -13.7 mT is the EDMR and the response near 0 mT is the NZF. We see that the NZF and EDMR responses is very sensitive to the differences in processing. The NO anneal has a profound impact on the size and line shape of both spectra. Previous EDMR measurements show that NO anneals significantly reduce the EDMR response [9]. This is due to N passivation of interface states. CP measurements show that the NO annealed sample has an average areal interface defect density of about a factor of 10 lower than the as-grown sample. It appears the anneals have a similar effect on the NZF response, which suggests similar physics are involved.

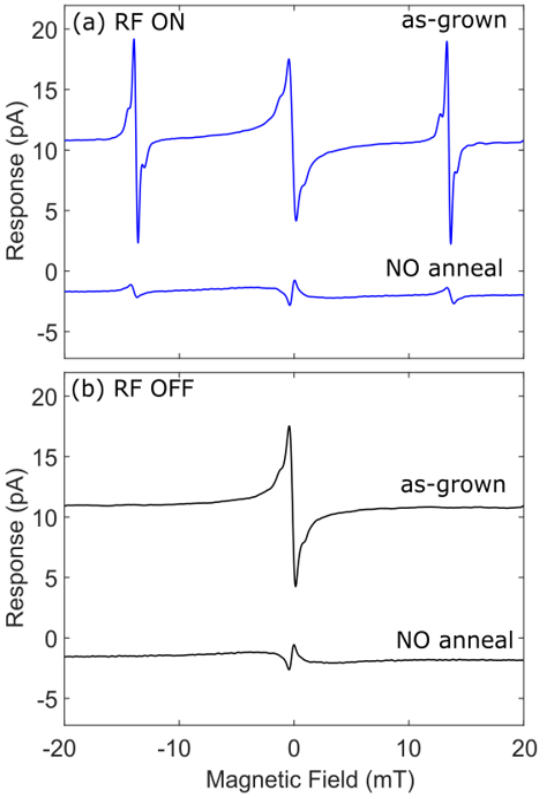


Figure 1. (a) NZF and EDMR SDCP and (b) only NZF measurements from the as-grown and NO annealed samples. Modulation amplitude was 0.15 mT and $f_{CP}$ was 1 MHz. All spectra are offset from 0 pA for easier comparison.

We also find that the line shape is significantly different for the NO and as-grown sample NZF responses. Fig. 2 shows the integral of the two NZF response amplitudes normalized to 1. Compared to the as-grown MOSFET spectrum, the MOSFET which received the NO anneal displays a much broader line shape and has a distinct sharp dip very near zero mT, which manifests as a sharp line in the derivative shown in the inset in Fig. 2. The overall increase in broadening between the as-grown and NO annealed spectra is at least in part due to hyperfine interactions between nearby N atoms and the observed trap. We know this from previous EDMR measurements which find that a great majority of the observed interface defects are very close, likely third-nearest neighbors away from N introduced by the NO anneal [10]. Previous magnetoresistance measurements have also found the increased hyperfine coupling broadens the NZF response [15]. Although the broadening is also observed in the EDMR, the NZF broadening is much more significant.

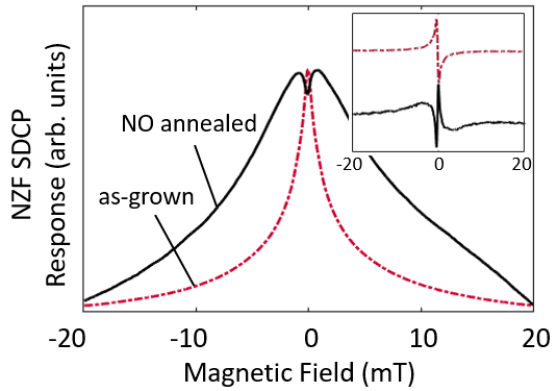


Figure 2. Amplitude normalized integral of the NZF SDCP measurements from the as-grown and NO annealed samples. Modulation amplitude was 0.15 mT and $f_{CP}$ was 1 MHz. The assymetry in the "NO annealed" trace is likely due to an artifact in our measurement system. Inset shows the measured derivatives of each sample with amplitudes normalized to 1.

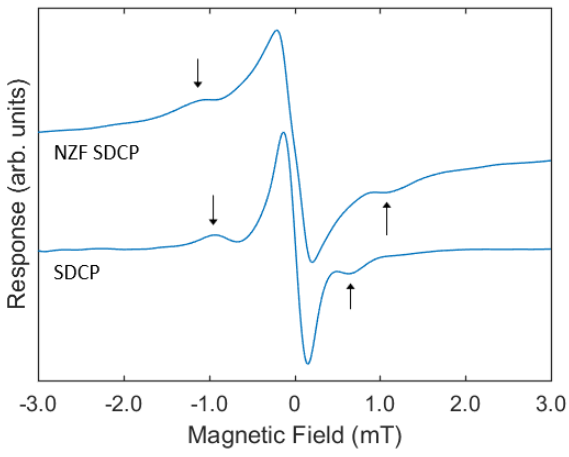


Figure 3. Comparison of NZF and ULRF (about 370 MHz) SDCP measurements. Arrows draw attention to the peaks in both spectra. Modulation amplitude was 0.2 mT and $f_{CP}$ was 1 MHz. The ULRF SDCP is shifted to 0 for easier comparison. We note that the asymmetry in the doublet signal in related to the centerline for the ULRF SDCP measurements are due to the Breit-Rabit effect [19]. Spectra are offset from 0 (y-axis) and amplitude normalized to 1 for easier comparison of line shape.

We also observe a side peak about 1 mT from 0 mT in the as-grown NZF spectra. A similar pattern appears in the EDMR, as illustrated in Fig. 3. These peaks are likely due to resolved hyperfine interactions involved with a defect called the 10.4 Gauss doublet, a H-complexed oxygen vacancy. Oxygen vacancy defects are known to be involved with bias temperature instabilities in $Si/SiO_2$ and $SiC/SiO_2$ devices [16], [17].As mentioned previously, observation of these resolved hyperfine interactions are important because they are often required for definitive defect identification in EPR and EDMR. Thus, the NZF measurement could very well be used to make defect identification. However, a thorough understanding of the NZF physics must be developed in order to realize the full potential of the NZF response.

To gain some insight into the physics involved in the NZF response, we made NZF and EDMR measurements as a function of $f_{CP}$. Figs. 4 and 5 show the amplitudes of the NZF and EDMR responses of the as-grown and NO annealed samples, respectively. The as-grown sample has a similar NZF and EDMR $f_{CP}$ dependence; they increase monotonically, then appear to saturate. This suggests that similar physics are involved in both responses. As mentioned previously, the NZF spectrum from the NO annealed sample shows two distinct responses. The broad response and the sharp response (or sharp dip) near 0 mT. The broad NZF and the EDMR responses from the NO annealed sample show similar behavior. However, the sharp response increases linearly without saturating. It appears that similar physics are involved with the broad NZF and EDMR responses, but the origin of the sharp response is unknown. A thorough study must be undertaken to fully understand the origins of the sharp line, but it can be qualitatively explained as the result of two different hyperfine coupling constants. One from the N, and another presumably from the magnetic Si and/or C atoms [18].

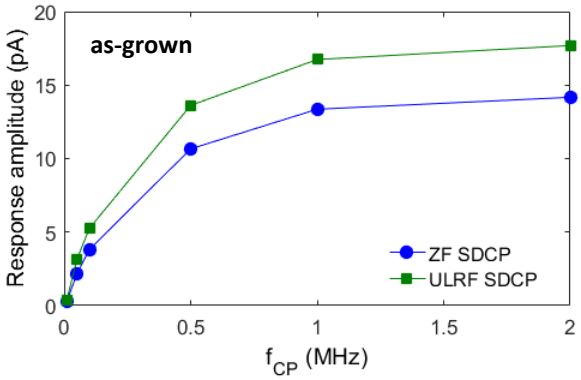


Figure 4. Comparison of NZF and ULRF (about 370 MHz) SDCP peak-to-peak amplitudes for the as-grown sample. Modulation amplitude was 0.15 mT.

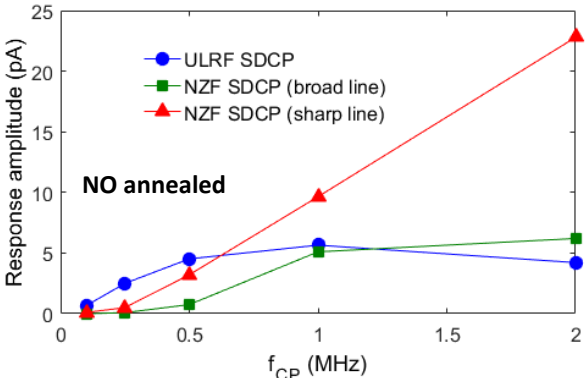


Figure 5. Comparison of NZF and ULRF (about 370 MHz) SDCP peak-to-peak amplitudes for the NO annealed sample. Modulation amplitude was 0.25 mT.

Our measurements strongly suggest that the NZF SDCP response could be a powerful tool to obtain atomic-scale physiochemical information about MOSFET interfaces. It could do so in a simple, inexpensive package compared to traditional EDMR. Thus, we integrate a NZF measurement system into a wafer probing station. This form factor is ideal for high-throughput device monitoring. Fig. 6a shows a picture of the wafer-level NZF spectrometer, Fig. 6b shows a schematic of the main parts of the system, and Fig. 6c shows a representative NZF SDCP measurement from a SiC MOSFET with a $SiO_2/Si_3N_4/SiO_2$ gate stack. The as-grown and NO-annealed samples were also measured (not shown), and the line shapes were not different from the traditional system. The measurements were made with the bottom plane of the electromagnet about 8 mm from the surface of the wafer. The nature of the single coil design introduces some magnetic field uniformity. However, the z-axis nonuniformity is negligible over the active sample area (<10 nm), and the x-y plane nonuniformity is good enough to resolve a 0.05 mT wide line, which is sharp enough to resolve all our NZF and EDMR

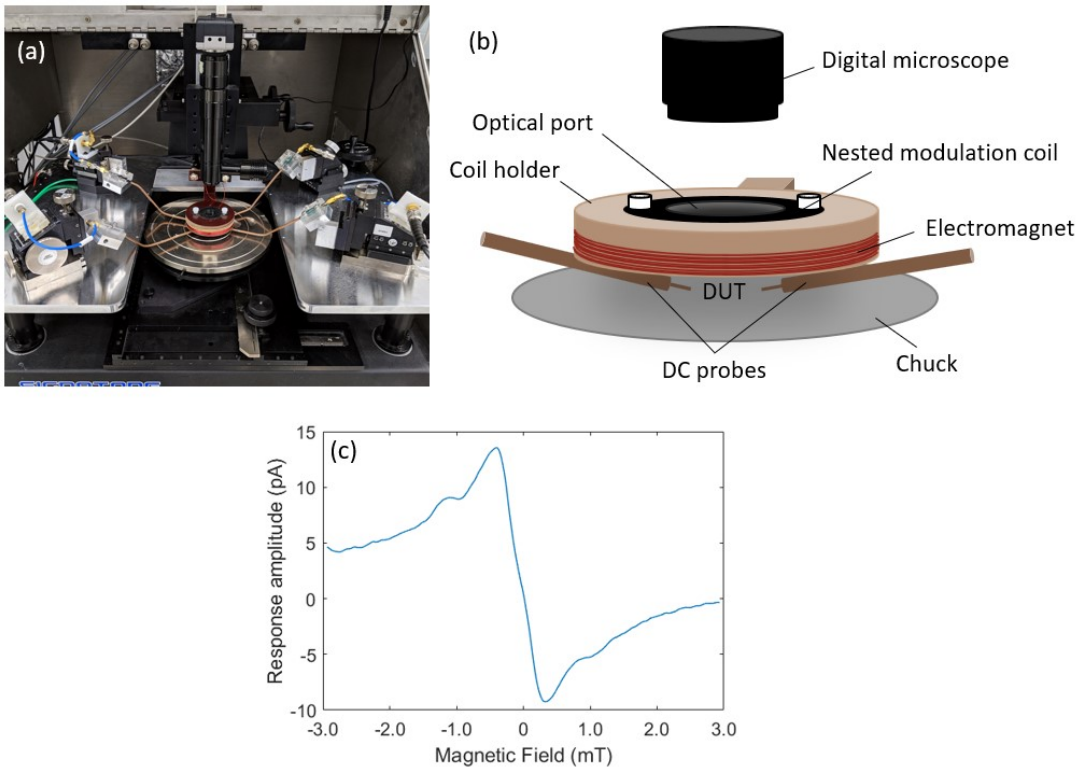


Figure 6. (a) is a photograph of the integrated wafer-prober and NZF measurement set-up. (b) is a cartoon illustration of the integrated sweep coil and its surroundings. (c) is the NZF SDCP from a 4H-SiC MOSFET with $SiO_2/S_3N_4/SiO_2$ gate stack. Modulation was 0.15 mT and $f_{CP}$ was 1 MHz.

line widths. In this sample, we observe the doublet signal that appears in the as-grown sample. This suggests that the $SiO_2$ oxygen vacancy plays a role at this MOSFET interface.

## Summary

NZF SDCP is a new approach to measure spin dependent charge capture events at MOSFET interfaces. We find that the measurement is very sensitive to NO anneals in SiC MOSFETs, thus can potentially be used to monitor processing changes in devices. We also likely resolve hyperfine interactions in the NZF measurements which means this approach could be a simple, cheap way to identify defects in MOSFET structures. We compare the NZF response to the EDMR response and find many similarities. It is likely that both involve similar physics. However, a deeper understanding of the theory and physics involved in this technique must be developed in order to realize its full potential. We integrate the NZF measurement system into a wafer probing station and demonstrate measurements on a 4H-SiC MOSFET.

## Acknowledgements

This paper describes objective technical results and analysis. Any subjective views or opinions that might be expressed in the paper do not necessarily represent the views of the U.S. Department of Commerce or the United States Government. Additionally, certain commercial equipment, instruments, or materials are identified in this paper to foster understanding. Such identification does not imply recommendation or endorsement by the National Institute of Standards and Technology, nor does it imply that the materials or equipment identified are necessarily the best available for the purpose.

## References

[1] T. Umeda *et al.*, "Behavior of nitrogen atoms in SiC-SiO2 interfaces studied by electrically detected magnetic resonance," *Appl. Phys. Lett.*, vol. 99, no. 14, pp. 8–11, 2011.

[2] C. J. Cochrane, P. M. Lenahan, and A. J. Lelis, "Identification of a silicon vacancy as an important defect in 4H SiC metal oxide semiconducting field effect transistor using spin dependent recombination," *Appl. Phys. Lett.*, vol. 100, no. 2, 2012.

[3] M. A. Anders, P. M. Lenahan, and A. J. Lelis, "Multi-resonance frequency spin dependent charge pumping and spin dependent recombination - Applied to the 4H-SiC/SiO2 interface," *J. Appl. Phys.*, vol. 122, no. 23, 2017.

[4] C. J. Cochrane, P. M. Lenahan, and A. J. Lelis, "An electrically detected magnetic resonance study of performance limiting defects in SiC metal oxide semiconductor field effect transistors," *J. Appl. Phys.*, vol. 109, no. 1, 2011.

[5] H. Itoh, N. Hayakawa, I. Nashiyama, and E. Sakuma, "Electron spin resonance in electron-irradiated 3C-SiC," *J. Appl. Phys.*, vol. 66, no. 9, pp. 4529–4531, Nov. 1989.

[6] N. T. Son *et al.*, "Electron-paramagnetic-resonance studies of defects in electron-irradiated p-type 4H and 6H SiC," *Phys. B Condens. Matter*, vol. 273–274, pp. 655–658, 1999.

[7] D. J. McCrory *et al.*, "Slow- and rapid-scan frequency-swept electrically detected magnetic resonance of MOSFETs with a non-resonant microwave probe within a semiconductor wafer-probing station," *Rev. Sci. Instrum.*, vol. 90, no. 1, 2019.

[8] R. Kosugi, T. Umeda, and Y. Sakuma, "Fixed nitrogen atoms in the SiO2/SiC interface region and their direct relationship to interface trap density," *Appl. Phys. Lett.*, vol. 99, no. 18, pp. 2009–2012, 2011.

[9] C. J. Cochrane, P. M. Lenahan, and A. J. Lelis, "The effect of nitric oxide anneals on silicon vacancies at and very near the interface of 4H SiC metal oxide semiconducting field effect transistors using electrically detected magnetic resonance," *Appl. Phys. Lett.*, vol. 102, no. 19, pp. 1–5, 2013.

[10] M. A. Anders, P. M. Lenahan, A. H. Edwards, P. A. Schultz, and R. M. Van Ginhoven,

"Effects of nitrogen on the interface density of states distribution in 4H-SiC metal oxide semiconductor field effect transistors: Super-hyperfine interactions and near interface silicon vacancy energy levels," *Journal of Applied Physics*, vol. 124, no. 18. 2018.

[11] J. S. Brugler and P. G. A. Jespers, "Charge pumping in MOS devices," *IEEE Trans. Electron Devices*, vol. 16, no. 3, pp. 297–302, Mar. 1969.

[12] G. Groeseneken, H. E. Maes, N. Beltran, and R. F. De Keersmaecker, "A Reliable Approach to Charge-Pumping Measurements in MOS Transistors," *IEEE Trans. Electron Devices*, vol. 31, no. 1, pp. 42–53, 1984.

[13] B. C. Bittel, P. M. Lenahan, J. T. Ryan, J. Fronheiser, and A. J. Lelis, "Spin dependent charge pumping in SiC metal-oxide-semiconductor field-effect-transistors," *Appl. Phys. Lett.*, vol. 99, no. 8, pp. 1–4, 2011.

[14] D. Kaplan, I. Solomon, and N. F. Mott, "Explanation of the Large Spin-Dependent Recombination Effect in Semiconductors.," *J Phys Lett*, vol. 39, no. 4, 1978.

[15] T. D. Nguyen *et al.*, "Isotope effect in spin response of π-conjugated polymer films and devices," *Nat. Mater.*, vol. 9, no. 4, pp. 345–352, 2010.

[16] P. M. Lenahan, "Atomic scale defects involved in MOS reliability problems," *Microelectron. Eng.*, vol. 69, no. 2–4, pp. 173–181, 2003.

[17] A. J. Lelis, R. Green, D. B. Habersat, and M. El, "Basic mechanisms of threshold-voltage instability and implications for reliability testing of SiC MOSFETs," *IEEE Trans. Electron Devices*, vol. 62, no. 2, pp. 316–323, 2015.

[18] C. R. Timmel, F. Cintolesi, B. Brocklehurst, and P. J. Hore, "Model calculations of magnetic field effects on the recombination reactions of radicals with anisotropic hyperfine interactions," *Chemical Physics Letters*, vol. 334, no. 4–6. pp. 387–395, 2001.

[19] G. Breit and I. Rabi, "Measurement of nuclear spin," Phys. Rev., vol. 38, no. 11, pp. 2082-2083, 1931.